Turbulent flow around a square cylinder: a comparison of RNG $k-\varepsilon$ and STD $k-\omega$ models

Marta Di Ridolfi (LinkedIn profile),
Ludovica D'Incà (LinkedIn profile),
Biagio Torsello (LinkedIn profile).

Abstract

In the present study the turbulent flow around a square cylinder is computed with the purpose of highlighting and analyzing the main differences between two turbulence models: RNG $k-\varepsilon$ and standard $k-\omega$. Moreover, the treatment used near the walls is based on the *wall functions approach*. The numerical results are compared with data and results proposed in the literature. In all the computations mentioned in this paper the body geometry is kept fixed ($B/D = 1$), as well as the computational grid; furthermore, unsteady flows with zero incidence attack angle, $Re = 22000$, $It = 2\%$ (taken from experimental setups done by Lyn and Rodi [1]) and $L_T = 0.5B$ are numerically simulated. Lastly, the flow field around the square cylinder is analyzed in 2D only.

1. Introduction

The aerodynamic characteristics of rectangular cylinders is becoming, as time passes, more relevant. This is because in order to build and design long-span bridges and civil structures, for example, the dynamic response of these bodies under unsteady wind loads has a great impact that needs to be taken into account. Moreover, the scientific community has been drawn by this specific problems since Okajima's [2] and Tamura's [3] experimental works. Computational Fluid Dynamics (CFD) technology provides an approach to investigate the aerodynamic characteristics previously mentioned. The paper is organised in three main sections: firstly the computational models and the structure of the numerical solutions are introduced, followed by the numerical results obtained from the simulations, which are then compared with the ones present in literature; in conclusion the most relevant results are highlighted.

2. Computational solution elements

This section introduces the cornerstones on which the computational solution relies on.

2.1. Turbulent flow models

The turbulent flow around the obstacle is modelled by the Reynolds Averaged Navier Stokes equations (RANS) statistical approach:

$$\begin{cases} \dfrac{\partial \bar{u}_i}{\partial x_i} = 0 \\ \\ \dfrac{\partial \bar{u}_i}{\partial t} + \bar{u}_j \dfrac{\partial \bar{u}_i}{\partial x_j} = -\dfrac{1}{\rho}\dfrac{\partial \bar{p}}{\partial x_i} + \dfrac{\partial}{\partial x_j}\left[\nu \cdot \left(\dfrac{\partial \bar{u}_i}{\partial x_j} + \dfrac{\partial \bar{u}_j}{\partial x_i}\right)\right] - \dfrac{\partial}{\partial x_j}\left(\overline{u_i' u_j'}\right) \end{cases}$$

where ν is the kinematic viscosity and $\bar{u}_i$, $\bar{p}$ are the ensemble means of u_i and p, respectively.

The Reynolds stress term is modelled using the Boussinesq assumption:

$$\overline{u_i' u_j'} = \nu_T \left(\frac{\partial \bar{u}_i}{\partial x_j} + \frac{\partial \bar{u}_j}{\partial x_i} \right) \quad ,$$

in which ν_T is the eddy viscosity. Two different approaches for closing the system lead to the RNG $k-\varepsilon$ and STD $k-\omega$ turbulence models:

- RNG $k-\varepsilon$:

$$\nu_T = C_\mu \frac{k^2}{\varepsilon} \quad ,$$

where k is the turbulent kinetic energy $\left[\frac{m^2}{s^2}\right]$ and ε is the rate of dissipation of turbulent kinetic energy $\left[\frac{m^2}{s^3}\right]$. The two transport equations for k and ε are:

$$\frac{\partial k}{\partial t} + \frac{\partial \bar{u}_j k}{\partial x_j} = \frac{\partial}{\partial x_j} \left[\left(\frac{\nu_T}{\sigma_k} + \nu \right) \frac{\partial k}{\partial x_j} \right] + \nu_T \left(\frac{\partial \bar{u}_i}{\partial x_j} + \frac{\partial \bar{u}_j}{\partial x_i} \right) \frac{\partial \bar{u}_i}{\partial x_j} - \varepsilon \tag{1}$$

(2)

$$\frac{\partial \varepsilon}{\partial t} + \frac{\partial \bar{u}_j \varepsilon}{\partial x_j} = \frac{\partial}{\partial x_j} \left[\left(\frac{\nu_T}{\sigma_\varepsilon} + \nu \right) \frac{\partial \varepsilon}{\partial x_j} \right] + \frac{\varepsilon}{k} C_{\varepsilon 1} \nu_T \left(\frac{\partial \bar{u}_i}{\partial x_j} + \frac{\partial \bar{u}_j}{\partial x_i} \right) \frac{\partial \bar{u}_i}{\partial x_j} - \frac{\varepsilon}{k} C^*_{\varepsilon 2} \varepsilon \tag{3}$$

- STD $k-\omega$ model:

$$\nu_T = \frac{k}{\omega} \quad , \quad \omega = \frac{1}{\beta^*} \frac{\varepsilon}{k} \quad , \tag{4}$$

in which ω is the specific rate of dissipation $[s^{-1}]$ and β^* is a constant. The transport equation for ω is:

$$\frac{\partial \omega}{\partial t} + \frac{\partial \bar{u}_j \omega}{\partial x_j} = \frac{\partial}{\partial x_j} \left[\left(\frac{\nu_T}{\sigma_\omega} + \nu \right) \frac{\partial \omega}{\partial x_j} \right] + \frac{\omega}{k} C_{\omega 1} \cdot \left(\frac{\partial \bar{u}_i}{\partial x_j} + \frac{\partial \bar{u}_j}{\partial x_i} \right) \frac{\partial \bar{u}_i}{\partial x_j} - C_{\omega 2} \omega^2$$

The last term in (1) becomes $\beta^* \omega k$ with following changes in the value of the constants.

All the coefficients $C_{..}$, $\sigma_.$, β^* that appear in the equations just mentioned are empirical values, whereas $C^*_{\varepsilon 2}$ is a function of two different characteristic times of the flow. The boundary and initial conditions of the models are specified in the next section, after the description of the computational domain.

2.2. Computational grid and numerical schemes

The origin of the cartesian axes corresponds with the stagnation point and the computational domain covers $-15B \sim 30B$ in the streamwise direction and $-15B \sim 15B$ in normal direction. Hybrid grids (quadrangular and triangular) are used in the whole computational domain, in particular a quadrangular structured and orthogonal mesh is used around the body, in correspondence with the physical boundary layer, in order to have a better approximation of the flow that is characterised by high gradient values in the so said area.

The chosen boundary conditions for the problems are:

- along the inlet:
  - $U_x = 1$ and $U_y = 0$, where U_x is the x-component of the velocity and U_y the y-component;
  - $It = 2\%$ (see [1]);
  - $L_T = 0.5B$ (an assumption that constitutes a degree of uncertainty of the model);

From these values it is immediate to calculate the inlet conditions for $k = \frac{3}{2}(U_x It)^2$, $\varepsilon = 0.01\frac{k^{3/2}}{L_T}$ (in the $k-\varepsilon$ model) and the one for ω using the right equation in (4) (in the $k-\omega$ model);

- along the outlet: $p_{rel} = 0$ and for k, ε, ω the same conditions as the ones imposed along the inlet;
- on all the edges: no slip condition.

The initial conditions are uniform, obtained from repeating the boundary conditions for the primitive variables in all the computational domain. The simulation covers $T = 8000$ time units in order to allow the statistical analysis of the flow to be computed only later than becoming periodic, after a first transient solution. The latter is related to the initial conditions that are not consistent with the phenomenological behaviour expected in the current study. Numerical solutions in this paper is found using a commercial CFD code, ANSYS FLUENT, which implements the finite-volume method to solve the governing equations. The numerical schemes chosen to solve the problem are: PISO for the coupling of pressure and velocity, QUICK for the spatial discretization of convective terms, CDS for the diffusive terms and a second order implicit Euler's scheme for time discretization in which the time unit is set to $\Delta t = 2 \cdot 10^{-2}$.

3. Numerical results

In this section the influence of the turbulence models is investigated following Lyn's [1] approach that consists on dividing the shedding period into 20 phases, after overcoming the transient, mentioned in section 2.2. The latter allows to compute the time average value of the parameters, which is the one the following results refer to.

3.1. Integral parameters

In the following table some integral parameters (St, $\bar{C}_D$, $\tilde{C}_L$ and $\tilde{C}_D$) are displayed.

Turbulence models			
	RNG $k-\varepsilon$	standard $k-\omega$	Experiments/LES computation
St	0.138	0.136	Lyn [1]: 0.135
$\bar{C}_D$	1.902	2.018	Lyn [1]: $2.05-2.23$
$\tilde{C}_L$	0.988	1.379	Murakami [4]: 1.60
$\tilde{C}_D$	0.0394	0.136	Murakami [4]: 0.13

Table 1: Integral parameters

In this problem the Strouhal number is equivalent to the frequency of the complete detachment of the shedding vortex and both models estimate it well, but the $k-\omega$ one is closer to Lyn's [1] one. It is clear that the $k-\varepsilon$ model underestimates the other integral parameters that are the time mean and the fluctuating aerodynamic resistance ($\bar{C}_D$ and $\tilde{C}_D$) and the fluctuating aerodynamic lift on the body ($\tilde{C}_L$). From an engineering point of view, underestimating the latter could be dangerous since it is better working in safety conditions. For what concerns the last remark, the standard $k-\omega$ model, compared with the literature values, gives better results.

3.2. Time averaged distributions and phase dependent results

The first parameters taken into account are the time mean pressure coefficient and the *rms* pressure coefficient, which can be viewed in figures 1a and 1b, respectively.

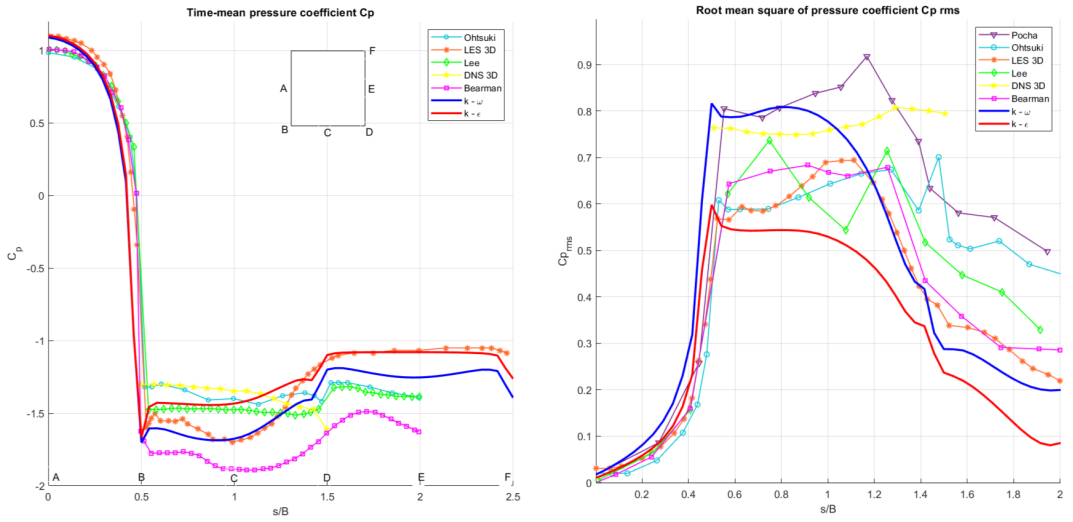

(a) Time mean pressure coefficient

(b) *Rms* of the pressure coefficient

Looking at the time average of the pressure coefficient graph 1a it is clear that both models are consistent with the data found in literature. Moreover $k-\varepsilon$ and $k-\omega$ are comparable between $0s/B \sim 0.5s/B$, but the same can not be said after $0.5s/B$ where there are higher values of $\bar{C}_p$ for what concerns the $k-\varepsilon$ results and lower ones for the $k-\omega$ ones. A difference is also noticeable in the *rms* graph 1b where the $k-\omega$ model reaches high values, closer to Pocha's experimental data [5], and the $k-\varepsilon$ model is found to be the lower curve with smaller distance from Lee [6], Ohtsuki [7] and Bearman [8] values. $\bar{C}_p$ is expected to be equal to one where the stagnation point is, followed by a decay after the separation of the flow; after that, the value of the parameter should remain approximately constant, since the basal surface of the body is limited. This phenomenon is well represented by both turbulence models, where can be highlighted that since the separation point corresponds with the leading edge vertices, the pressure coefficient decay is very steep. Furthermore, it is shown that the underestimating of $\tilde{C}_L$ previously mentioned for the $k-\epsilon$ model is due to the underestimate of the *rms* of the pressure coefficient with respect to the literature and $k-\omega$ data (1b).

The second parameter in analysis is the averaged streamwise velocity along the centerline ($y=0$).

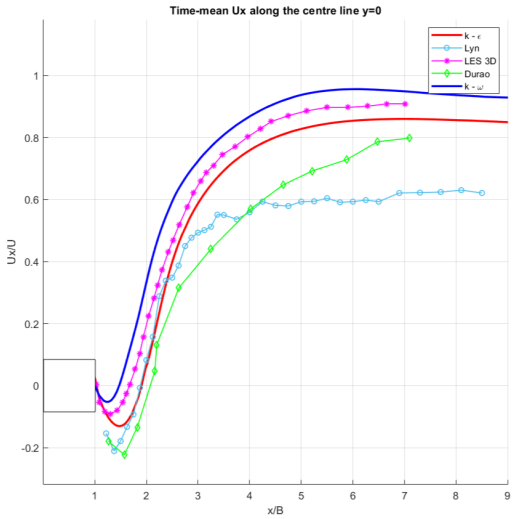

Figure 2: Time averaged U_x along the centerline $y=0$

The results show that both models correctly capture the negative velocity in the recirculation area, found between $1 \leq x/B \leq 2$. $k-\varepsilon$ model fits better Lyn [1] and Durao [9] data, while $k-\omega$ underestimate (considering the absolute value) the backward velocity. In addition the recirculation length is understimated by the $k-\omega$ approach, whereas for the $k-\varepsilon$ it is exactly the same as Lyn's

[1] one. Looking at the right side of the graph, the flow velocity should physically, as distance from the body increases, reach the initial unit value. This behaviour is better represented by the $k-\omega$ model, but to have more precise values and data to better compare the two models, the domain after the body should be extended more.

The third parameter studied is the instantaneous x-velocity along the line $x = 1$.

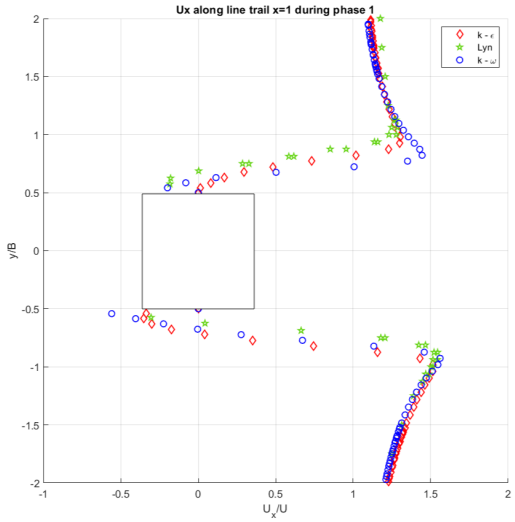

(a) U_x along the line trail, phase 1

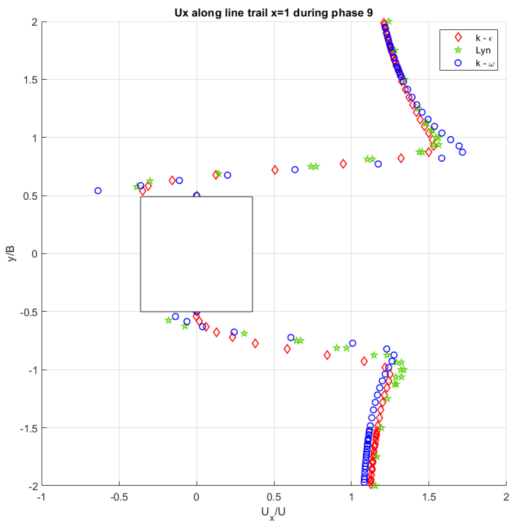

(b) U_x along the line trail, phase 9

The graphs 3a and 3b refer to the instantaneous x-velocity during the first and ninth phases. It is clear that the results from the simulations are consistent with the one given in literature: there are not visible differences between the models. Moreover the velocity along the trail is expected to be symmetric and null on the body edges in order to satisfy the no-slip condition. The parameter should assume negative values in the recirculation area and unit value as the flow distance itself from the body. All these physical aspects are well captured from both turbulence models according to Lyn's data [1].

The fourth parameter is the time mean of the kinetic energy along the center line.

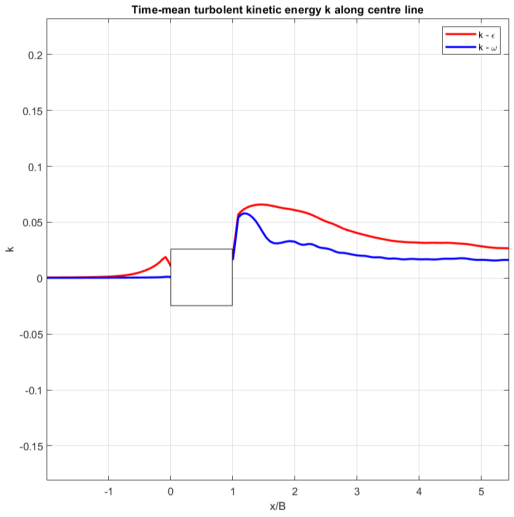

(a) Kinetic energy along the center line, time mean

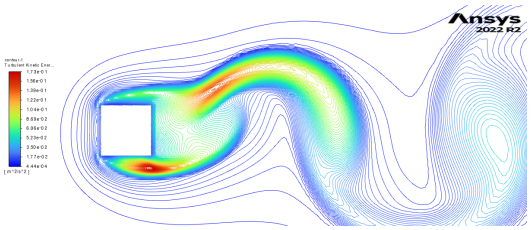

(b) Kinetic energy contour lines for $k-\varepsilon$, phase 1

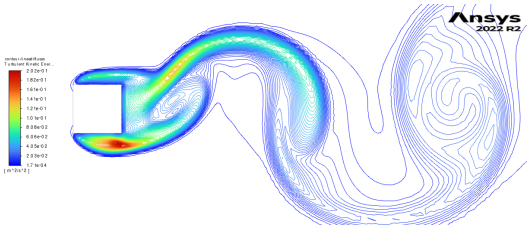

(c) Kinetic energy contour lines for $k-\omega$, phase 1

This parameter analysis is limited to the two turbulence models only. The graphs above show that the time average of the kinetic energy of the flow before the body is null, as it should, for the $k-\omega$ model. The RNG $k-\varepsilon$ model, instead, shows a production of k in the stagnation region, even if much

lower than the one observed for the standard $k-\varepsilon$ model (see [10]). Furthermore, both the models underpredict the level of turbulent kinetic energy behind the cylinder, as reported in [10] where the simulations are compared with Lyn's experimental data. In figures 4b and 4c, which refers to the instantaneous variable during phase one, this behaviour is also highlighted: contours lines can be seen before the body in figure 4b which represents the RNG $k-\varepsilon$ model and no contour lines are present for the $k-\omega$ one.

4. Conclusions

Time-dependent numerical simulations of an unsteady flow with zero attack angle around a square cylinder ($B/D = 1$) at Reynolds number 22000, $It = 2\%$ and $L_T = 0.5B$ has been carried out. The study aim was to describe the characteristics and main differences between the RNG $k-\varepsilon$ and standard $k-\omega$ turbulence models. Overall, the two models give approximations that meet the ones from literature. In general the simulated aerodynamic behaviour is the one expected given the specific regime of the problem, as it can be seen for most of the time averaged and instantaneous values of the variables ($\bar{C}_P$, averaged and instantaneous U_x). Some remarks can be made for what concerns the time average kinetic energy parameter for both models, which underestimate the values in the wake with respect to the experimental data. Moreover the RNG $k-\varepsilon$ model predicts an unrealistic phenomenon, which is the production of k in the stagnation area. From the analysis of the parameters $\bar{C}_p$, U_x, and k (both averaged and instantaneous) it is difficult to determine which of the two models suits better the problem. On the other hand, looking at the study of the integral parameters it is clear that the values provided by $k-\omega$ turbulence model are more comparable with the data in literature than the one given from the RNG $k-\varepsilon$ model. As it was mentioned in the previous section, this is particularly important for the behaviour of the fluctuating component of the aerodynamic lift.

References

[1] D. Lyn, W. Rodi, The flapping shear layer formed by flow separation from the forward corner of a square cylinder, Journal of fluid Mechanics 267 (1994) 353–376.

[2] A. Okajima, Strouhal numbers of rectangular cylinders, Journal of Fluid mechanics 123 (1982) 379–398.

[3] T. Tamura, Y. Ito, Aerodynamic characteristics and flow structures around a rectangular cylinder with a section of various depth/breadth ratios, Journal of Structural and Construction Engineering (Transactions of Architectural Institute of Japan) 486 (1996) 153–162.

[4] S. Murakami, A. Mochida, On turbulent vortex shedding flow past 2d square cylinder predicted by cfd, Journal of Wind Engineering and Industrial Aerodynamics 54 (1995) 191–211.

[5] J. J. Pocha, On unsteady flow past cylinders of square cross-section, Ph. D. Thesis, Department of Aeronautics, Queen Mary College.

[6] S. Lee, Unsteady aerodynamic force prediction on a square cylinder using k- ε turbulence models, Journal of Wind Engineering and Industrial Aerodynamics 67 (1997) 79–90.

[7] Y. Ohtsuki, Wind tunnel experiments on aerodynamic forces and pressure distributions of rectangular cylinders in a uniform flow, in: Proc. 5th Symp. on Wind effects on structures, 1978, pp. 169–175.

[8] P. Bearman, E. Obasaju, An experimental study of pressure fluctuations on fixed and oscillating square-section cylinders, Journal of Fluid Mechanics 119 (1982) 297–321.

[9] D. Durao, M. Heitor, J. Pereira, Measurements of turbulent and periodic flows around a square cross-section cylinder, Experiments in fluids 6 (5) (1988) 298–304.

[10] R. t. Franke, W. Rodi, Calculation of vortex shedding past a square cylinder with various turbulence models, in: Turbulent Shear Flows 8: Selected Papers from the Eighth International Symposium on Turbulent Shear Flows, Munich, Germany, September 9–11, 1991, Springer, 1993, pp. 189–204.